H-600 electron microscope, operating at 75 kV; N = 8 for each condition.
15. Unpublished ultrastructural observations from eight control explants.
16. M. Anniko, *Anat. Embryol.* **166**, 335 (1983); D. J. Lim and M. Anniko, *Acta Oto-Laryngol. Suppl.* **422**, 1 (1985); M. Lavigne-Rebillard and R. Pujol, *Anat. Embryol.* **174**, 396 (1986); M. Lenoir, J.-L. Puel, R. Pujol, *ibid.* **175**, 477 (1987).
17. M. Kessel, *Development* **115**, 487 (1992).
18. P. Dolle, E. Ruberte, P. Leroy, G. Morris-Kay, P. Chambon, *ibid.* **110**, 1133 (1990).
19. K. J. Balak, J. T. Corwin, J. E. Jones, *J. Neurosci.* **10**, 2502 (1990).

20. We thank A. Chalazonitis, D. Frenz, and R. J. Ruben for critical review and helpful suggestions. Supported by National Institute on Deafness and Other Communication Disorders grant DC00088 to T.R.V. and a Fond National de la Recherche Scientifique grant to P.P.L. and G.M. P.P.L. is supported by the Fondation Leon Fredericq of the Faculty of Medicine, University of Liège. The ultrastructure facility and H.S. are supported by National Institute of Neurological Diseases and Stroke neuropathology training grant NS07098.

30 October 1992; accepted 24 February 1993

Linkage on Chromosome 3 of Autoimmune Diabetes and Defective Fc Receptor for IgG in NOD Mice

Jan-Bas Prins, John A. Todd, Nanda R. Rodrigues, Soumitra Ghosh, P. Mark Hogarth, Linda S. Wicker, Erin Gaffney, Patricia L. Podolin, Paul A. Fischer, Anna Sirotina, Laurence B. Peterson

A congenic, non-obese diabetic (NOD) mouse strain that contains a segment of chromosome 3 from the diabetes-resistant mouse strain B6.PL–*Thy-1*^{a} was less susceptible to diabetes than NOD mice. A fully penetrant immunological defect also mapped to this segment, which encodes the high-affinity Fc receptor for immunoglobulin G (IgG), FcγRI. The NOD *Fcgr1* allele, which results in a deletion of the cytoplasmic tail, caused a 73 percent reduction in the turnover of cell surface receptor–antibody complexes. The development of congenic strains and the characterization of Mendelian traits that are specific to the disease phenotype demonstrate the feasibility of dissecting the pathophysiology of complex, non-Mendelian diseases.

Complex diseases such as autoimmune, insulin-dependent diabetes mellitus (IDDM) (*1–4*), hypertension (*5*), and epilepsy (*6*) are largely determined by a number of gene effects. The NOD mouse strain spontaneously develops IDDM (*7*), which is determined by at least nine unlinked loci [*Idd-1* through *Idd-9* (*1, 2, 8*)]. With the exception of *Idd-1*, which is encoded by genes within the major histocompatibility complex (MHC) on chromosome 17, no individual locus appears to be absolutely essential for disease onset. Heterozygosity even at the MHC has a low, but significant penetrance that makes fine mapping by standard linkage analysis impractical (in the absence of any obvious candidate genes) (*1–4*). Proof that any of the non-MHC loci encode significant effects and progress in fine mapping depend on the demonstration that NOD strains that are congenic for chromosomal regions encoding diabetes-resistant alleles are actually less susceptible to disease.

Idd-3, which is linked to both diabetes and insulitis, was mapped to a 48–centimorgan (cM) interval on chromosome 3, approximately between *D3Nds6* [interleukin-2 (*Il-2*)] and *D3Nds9* (*Adh-1*) (*1*). In this 48-cM interval, the marker loci *D3Nds7* [*Cacy* (*9*)], *D3Nds11* [*Fcgr1* (*10*)], and *D3Nds8* (*Tshb*), which are in a 7-cM region, show strong linkage to diabetes and insulitis (Table 1). These backcross data do not, however, permit assignment of the disease locus within this 7-cM interval or even to an adjacent interval. In order to fine map the disease locus and assess the role of the chromosomal region encompassing these three marker loci in diabetes, we measured the frequency of disease in the NOD.B6.PL–*Thy-1*^{a}–*D3Nds7 D3Nds8* (NOD.*D3Nds7 D3Nds8*) congenic strain, which contains a segment of chromosome 3 from B6.PL–*Thy-1*^{a} in the homozygous state. The cumulative frequency of diabetes, as compared with cohorts of male and female NOD mice, was reduced significantly in both male ($P < 0.0001$) and female ($P < 0.0001$) congenic mice (Fig. 1, A and B). We obtained further evidence that this segment, and not a region on a different chromosome, is the cause of the reduction in diabetes frequency by demonstrating linkage between chromosome 3 and diabetes in a backcross analysis (*11*). Statistical analyses of backcross data (*3*) and the frequency of diabetes in other congenic strains encompassing different regions of chromosome 3 (*4*) indicate that *Idd-3* is encoded by two or more distinct chromosome 3 loci, one of which is in the *D3Nds7-D3Nds8* region. The occurrence of diabetes in the NOD.*D3Nds7 D3Nds8* congenic strain shows that the NOD alleles of genes in this region are not essential for disease development but do contribute significantly.

Another approach to the dissection of a complex disease is to identify Mendelian phenotypes that are caused by single, fully penetrant genes that can be mapped easily and precisely and that might indicate candidate genes (*12*). We have identified such a trait in NOD mice. After injection of complete Freund's adjuvant (CFA), the number of peripheral blood cells expressing Mac-1, an integrin molecule present on macrophages, monocytes, and neutrophils (*13*), increased in both NOD (Fig. 2A) and nondiabetic strains such as C57BL/10SnJ (B10) (Fig. 2B). A portion of Mac-1$^+$ cells in NOD (Fig. 2, C and E) but not in B10 (Fig. 2D) mice bound a monoclonal antibody (MAb) to immunoglobulin G2a (IgG2a). The expression of this IgG2a$^+$ phenotype was unrelated to *Idd-1* because NOD.B10–*H-2*^{b} mice (NOD.*H-2*^{b}) (*14*) also developed this trait (Fig. 3).

The IgG2a$^+$ phenotype was inherited in backcross and F_2 progeny as a single gene dominant trait: 70 out of 129 or 54% of the progeny from the backcrosses (B6.PL–*Thy-1*^{a}

J.-B. Prins, J. A. Todd, N. R. Rodrigues, S. Ghosh, Nuffield Department of Surgery, University of Oxford, John Radcliffe Hospital, Headington, Oxford OX3 9DU, United Kingdom.
P. M. Hogarth, Austin Research Institute, Kronheimer Building, Austin Hospital, Heidelberg 3084, Australia.
L. S. Wicker and P. L. Podolin, Autoimmune Diseases Research, Merck Research Laboratories, Rahway, NJ 07065.
E. Gaffney and L. B. Peterson, Department of Cellular and Molecular Pharmacology, Merck Research Laboratories, Rahway, NJ 07065.
P. A. Fischer and A. Sirotina, Immunology Research, Merck Research Laboratories, Rahway, NJ 07065.

Table 1. Linkage of *D3Nds11* (*Fcgr1*) and flanking marker loci to insulitis and diabetes (*40*). He, heterozygous; Ho, NOD homozygous.

Marker locus	Recombination fraction (SE)	Insulitis He:Ho	χ^2	Diabetes He:Ho	χ^2
D3Nds7 (*Cacy*)		31:58	8.2*	22:84	36.3***
D3Nds11 (*Fcgr1*)	0.031 (0.015)	27:61	13.1**	24:82	31.7***
D3Nds8 (*Tshb*)	0.039 (0.017)	32:57	7.0*	25:81	29.6***

*$P < 10^{-2}$. **$P < 10^{-3}$. ***$P < 10^{-4}$.

× NOD)F_1 × B6.PL–*Thy-1*^{a} or [B10.NOD–*H-2*^{g7} (B10.*H-2*^{g7}) × NOD]F_1 × B10.*H-2*^{g7} expressed the phenotype as did 34 out of 44 or 77% of (B10.*H-2*^{g7} × NOD)F_2 mice. Using 58 locus-specific microsatellites (*15*) across the genome and DNA from 129 phenotyped first backcross progeny, we mapped the gene to the *D3Nds7 D3Nds8* interval on chromosome 3 (Table 2) that contains the gene for the high-affinity Fc receptor for IgG (*Fcgr1*) (*16, 17*). We determined the NOD and B10 *Fcgr1* cDNA sequences (*18*). The B10 sequence was identical to the published murine sequence (*17*). The NOD coding sequence, however, has 24 single-base differences, 17 of which encode changes in the predicted amino acid sequence (*19*). A deletion of four bases creates a stop codon at position 337, which results in a cytoplasmic tail lacking 73 amino acid residues or about 75% of the total length. We developed a polymerase chain reaction (PCR)–based assay to detect this deletion in the backcross progeny (*10*). There was complete linkage between the mutation and the phenotype ($P < 10^{-4}$; Table 2). Further support for a direct causal effect of the mutant FcγRI came from the congenic strain B10.NOD–*H-2*^{g7} *D3Nds7 D3Nds8* (N_7F_3). This strain expresses the phenotype, which indicates that the segment of DNA near *D3Nds8*, which encodes the NOD *Fcgr1* allele, is sufficient to encode the defect (*4*). This segment is also necessary for expression of the phenotype because the reciprocal congenic strain NOD.*D3Nds7 D3Nds8* was normal (*4*). The other known FcγR genes are located on chromosome 1 (*20*), and *Fcgr1* is the only FcγR gene mapped to this region of chromosome 3 (*16, 17*). The NOD IgG2a$^+$ phenotype was dominant, but the results in Table 1 show that linkage of *Fcgr1* to insulitis and diabetes was due to increased homozygosity. Thus, one dose of the wild-type allele in heterozygous mice is sufficient for the normal function of FcγRI and provides protection from diabetes.

To test if NOD FcγRI results in defective processing of IgG2a, we measured the retention of FcγRI-IgG2a complexes on the surface of NOD.*H-2*^{b} and B10 cells. When freshly isolated cells from CFA-injected mice were incubated with fluorescein isothiocyanate (FITC)–labeled IgG2a (FITC-IgG2a), NOD.*H-2*^{b} cells bound little FITC-IgG2a (Fig. 3A; shaded) as compared with B10 cells (Fig. 3B; shaded), which is consistent with the possibility that NOD FcγRIs are already occupied with endogenous IgG. To remove endogenous IgG and facilitate binding with exogenous IgG2a in vitro, we first cultured NOD.*H-2*^{b} and B10 cells, after which both NOD.*H-2*^{b} (Fig. 3A; unshaded) and B10 cells (Fig. 3B; unshaded) showed distinct FITC-IgG2a binding, although the NOD cells were low-

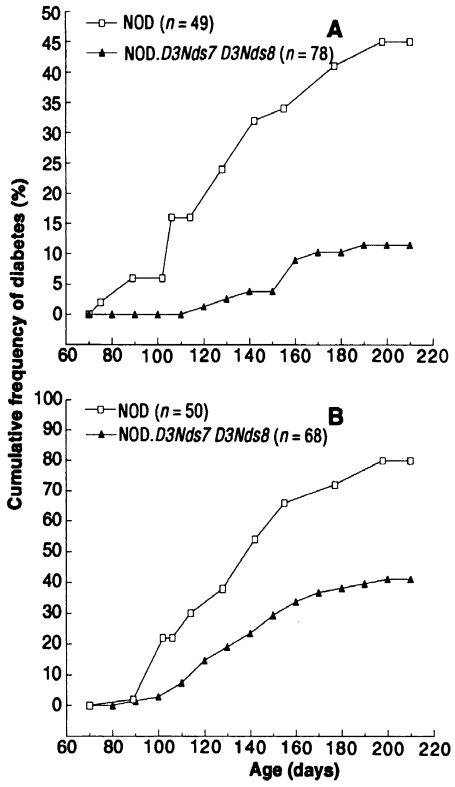

Fig. 1. The cumulative frequencies of diabetes by 210 days in NOD.*D3Nds7 D3Nds8* male (**A**) and female (**B**) mice as compared with the parental strain. The cumulative frequency is significantly reduced in both male (9 out of 78 versus 22 out of 49 NOD males; $\chi^2 = 18.2$, 1 df, $P < 0.0001$) and female (28 out of 68 versus 40 out of 50 NOD females; $\chi^2 = 17.8$, 1 df, $P < 0.0001$) congenic mice with a χ^2 test of independence (1 df). Breeding schemes of the congenic strains and information on marker loci are as described (*42*). None of the marker loci outside the congenic regions of chromosome 3 were of donor strain origin. This indicates that the other chromosome 3 regions and regions on other autosomes previously linked to diabetes are of NOD origin in the NOD.*D3Nds7 D3Nds8* strain.

Table 2. Linkage of chromosome 3 to the IgG2a$^+$ phenotype (*41*).

Marker locus	Recombination fraction (SE)	Discordant		χ^2
		IgG2a$^+$	IgG2a$^-$	
D3Nds6 (*Il-2*)		19/54	12/49	16.8*
D3Nds1	0.129 (0.033)	10/54	8/48	42.7*
D3Mit22	0.029 (0.017)	8/70	10/59	66.6*
D3Nds7 (*Cacy*)	0.108 (0.027)	2/70	2/59	113.4*
D3Nds11 (*Fcgr1*)	0.031 (0.015)	0/70	0/59	129.0*
D3Nds8 (*Tshb*)	0.039 (0.017)	3/70	2/59	109.7*
D3Nds9 (*Adh-1*)	0.216 (0.053)	6/30	8/27	14.6*

*$P < 0.0001$.

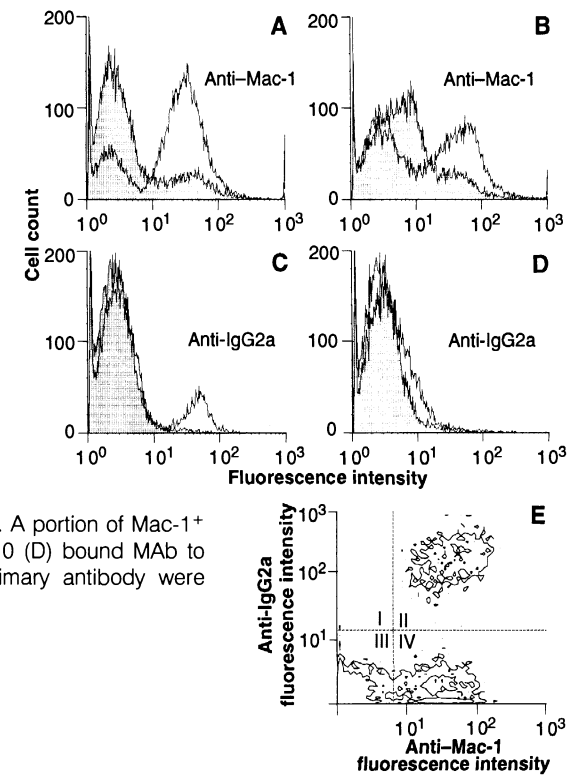

Fig. 2. Flow cytometric analysis of peripheral blood cells from NOD (**A**, **C**, and **E**) and B10 (**B** and **D**) mice. Mice were left untreated (shaded profiles) or immunized and boosted with CFA [unshaded profiles (*38*)]. Mac-1$^+$ cells (A, B, and E) were detected after incubation of peripheral blood cells with MAb to Mac-1 (anti–Mac-1) and FITC-conjugated MAb to rat κ. IgG2a$^+$ cells (C and D) were detected with anti-IgG2a and FITC-conjugated MAb to rat κ. In the two-color analysis (E); IgG2a$^+$ cells were detected with PE-conjugated antibody to IgG2a^b. Quadrants I to IV contain 1.3, 21.8, 51.8, and 25.1% of the population, respectively. Injection of CFA into NOD (A) and B10 (B) increases the number of Mac-1$^+$ cells. A portion of Mac-1$^+$ cells in NOD (C and E) but not in B10 (D) bound MAb to IgG2a. Isotype controls for each primary antibody were negative in all experiments.

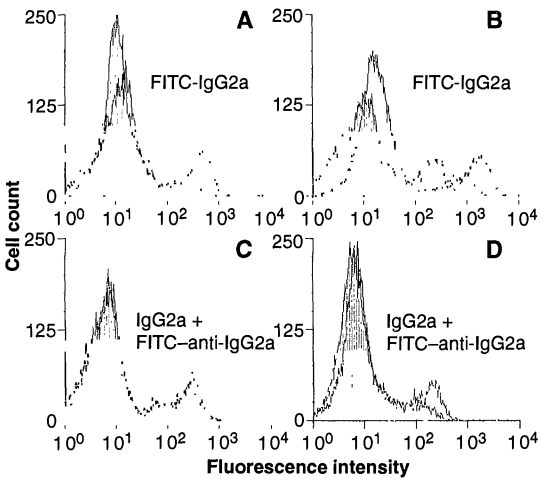

Fig. 3. Peripheral blood cells from CFA-injected (*39*) NOD.*H-2*^{b} (**A** and **C**) and B10 (**B** and **D**) mice were incubated with FITC-IgG2a immediately (A and B, shaded profiles) or after an overnight culture at 37°C (A and B, unshaded profiles). In the second half of the experiment, NOD.*H-2*^{b} (**C**) and B10 (**D**) peripheral blood cells were cultured for 16 hours at 37°C, incubated with IgG2a in vitro, washed, incubated on ice with FITC-conjugated antibody to IgG2a^b, washed, and then incubated for 0 min (C and D, unshaded profiles) and 5 min at 37°C (C and D, shaded profiles) (*38*).

er in intensity. To determine if receptor endocytosis was affected by the mutations, we cultured NOD.*H-2*^{b} (Fig. 3C) and B10 cells (Fig. 3D) as above and then incubated them with IgG2a and FITC-conjugated antibody to IgG2a. Subsequently, the cells were incubated at 37°C for 0 min and 5 min. After 5 min, B10 cells had internalized 70% of their FcγRI-IgG2a cell surface complexes, compared with only 19% by the NOD.*H-2*^{b} cells. Monomeric IgG2a was used in these experiments, which implicates the FcγRI for these effects and not the type II and III receptors (*21*), consistent with the genetic and sequencing data. The IgG2a$^+$ phenotype could be due to a defect in receptor internalization or in the dissociation of IgG2a from the receptor, which could be related to the NOD mutations in the extracellular domains (*19*).

Indirect evidence indicates that NOD macrophages are defective, but until now no specific defect had been described (*22*). Macrophages can express high concentrations of FcγRI (*23*) and are an essential component in the onset of insulitis and diabetes in NOD mice (*24*). Through their FcγRI, monocytes mediate antibody-dependent cellular cytotoxicity (ADCC) (*25*). ADCC activity in NOD mice has been shown to be higher than that in age-matched ICR mice, the strain from which NOD originated (*26*). We found that the ICR *Fcgr1* allele does not contain the deletion mutation (*27*). Furthermore, ADCC activity is elevated in human type 1 diabetics (*28*). The binding of immune complexes to human FcγRI induces the release of tumor necrosis factor–α (TNF-α) (*29*). This cytokine has potent effects on the frequency of diabetes in NOD mice (*30*) and on the viability of β cells in vitro (*31*). Human FcγRI is anchored to the cytoskeletal component actin-binding protein (*32*). After IgG binds to FcγRI, the actin-binding protein–FcγRI complex dissociates, which may allow the plasma membrane to become more flexible, suggesting a role for the actin-binding protein–FcγRI interaction in phagocytosis. Of 22 strains tested, only the high antibody responder Biozzi strain [AB/H; (*33*)], which produces high titers of antibodies like NOD (*34*), carries the *Fcgr1* nonsense mutation (*35*). AB/H macrophages have membrane processes that are not present on macrophages from the low-responder Biozzi line (*36*). This AB/H phenotype may be caused by increased membrane flexibility as a result of the putative absence of the interaction between actin-binding protein and truncated FcγRI molecules. The introgression of smaller regions of chromosome 3 in congenic strains and functional analysis of the mutant FcγRI will define the possible role of FcγRI in diabetes and permit identification of disease susceptibility genes.

REFERENCES AND NOTES

1. J. A. Todd *et al.*, *Nature* **351**, 542 (1991).
2. R. J. Cornall *et al.*, *ibid.* **353**, 262 (1991).
3. M. A. McAleer *et al.*, in preparation; S. Ghosh *et al.*, in preparation.
4. L. S. Wicker and L. B. Peterson, unpublished data.
5. H. J. Jacob *et al.*, *Cell* **67**, 213 (1991); P. Hilbert *et al.*, *Nature* **353**, 521 (1991).
6. M. L. Rise, W. N. Frankel, J. M. Coffin, T. N. Seyfried, *Science* **253**, 669 (1991).
7. S. Makino *et al.*, *Exp. Anim.* **29**, 1 (1980); L. Castano and G. S. Eisenbarth, *Annu. Rev. Immunol.* **8**, 647 (1990); D. V. Serreze and E. H. Leiter, *J. Immunol.* **140**, 3801 (1988); N. Hatamori, K. Yokono, M. Hagata, K. Shii, S. Baba, *Diabetes* **39**, 1070 (1990).
8. M. Hattori *et al.*, *Science* **231**, 733 (1986); M. Prochazka, E. H. Leiter, D. V. Serreze, D. L. Coleman, *ibid.* **237**, 286 (1987); L. S. Wicker *et al.*, *J. Exp. Med.* **165**, 1639 (1987).
9. The dinucleotide repeat microsatellite $(CA)_{31}$, designated *D3Nds7*, was isolated from a cosmid containing *Cacy* and *Capl* [cosmid 6.11 from the 129 library, H. Lehrach, Imperial Cancer Research Fund (ICRF), London, United Kingdom]. PCR reactions were done with the flanking primers 5′-CACAGTGAGACCAAACTC-3′ and 5′-CTTGGCTGTTATAGTGTTTG-3′ for 35 cycles comprising 1.5 min at 94°C, 1 min at 55°C, and 0.5 min at 72°C, giving a product of 117 bp.
10. PCR primers to *Fcgr1* were 5′-GTCCCCAGTCATCAGCTCCTG-3′ and 5′-CGCTTCTAACTTGCTGAAAGGAA-3′, and the locus was designated as *D3Nds11*. PCR was done for 32 cycles comprising 1.5 min at 94°C, 1 min at 63°C, and 0.5 min at 72°C. *D3Nds11* has two alleles corresponding to PCR products of 188 or 184 bp.
11. NOD.*D3Nds6 D3Nds8* (N_6F_2) mice were produced by repetitive backcrosses of (NOD.B6.PL–*Thy-1*^{a} × NOD)F_1 mice to the NOD parent and selected for resistance to diabetes. The location of *D3Nds6* is in Table 2. After five backcross generations, this strain had a segment of chromosome 3 (at least 30 cM) from the donor strain. This region was made homozygous by selective intercrossing. To determine if this region of chromosome 3 was solely responsible for the diabetes resistance observed in the NOD.*D3Nds6 D3Nds8* strain, we performed linkage analysis of diabetes and insulitis using the backcross (NOD.*D3Nds6 D3Nds8* × NOD)F_1 × NOD. Linkage of diabetes and insulitis was observed only to chromosome 3. NOD.*D3Nds7 D3Nds8* (N_7F_2) congenic mice were derived from NOD.*D3Nds6 D3Nds8* congenic mice by one additional backcross during which a recombination event occurred between *D3Nds1* and *D3Nds7*.
12. N. Risch, *Science* **255**, 803 (1992).
13. T. K. Kishimoto *et al.*, *Adv. Immunol.* **46**, 149 (1989).
14. L. S. Wicker, B. J. Miller, P. A. Fischer, A. Pressey, L. B. Peterson, *J. Immunol.* **142**, 781 (1989); L. S. Wicker *et al.*, *J. Exp. Med.* **176**, 67 (1992).
15. J. M. Love, A. M. Knight, M. A. McAleer, J. A. Todd, *Nucleic Acids Res.* **18**; 4123 (1990); T. J. Aitman, C. M. Hearne, M. A. McAleer, J. A. Todd, *Mammalian Genome* 1, 206 (1991); C. M. Hearne *et al.*, *ibid.*, p. 273; R. J. Cornall, T. J. Aitman, C. M. Hearne, J. A. Todd, *Genomics* **10**, 874 (1991); M. A. McAleer *et al.*, *Mammalian Genome* **3**, 457 (1992); R. J. Cornall, J. M. Friedman, J. A. Todd, *ibid.*, p. 620.
16. M. H. Meisler and M. F. Seldin, *Mammalian Genome* 1, S42 (1991); R. J. Oakey, T. A. Howard, P. M. Hogarth, K. Tani, M. F. Seldin, *Immunogenetics* **35**, 279 (1992).
17. N. Osman, C. A. Kozak, I. F. C. McKenzie, P. M. Hogarth, *J. Immunol.* **148**, 1570 (1992).
18. RNA was isolated from spleen with guanidine thiocyanate, and cDNA was synthesized with standard methods. We designed primers to amplify the *Fcgr1* cDNA (5′-ATGATTCTTACCAGCTTTGGAGAT-3′ and 5′-AGAGTTGCATGCCATGGTCCC-3′). PCR reactions (100 μl) were done with biotinylated and nonbiotinylated primers in a Perkin-Elmer Thermocycler (Cetus) for 32 cycles comprising 1.5 min at 94°C, 1 min at 60°C, and 2 min at 72°C; after cycle 32 the reactions were incubated for a further 10 min at 72°C. Products were separated on a 1% agarose gel [1 × TAE (0.04 M tris-acetate and 0.001 M EDTA)], and the 1230-bp bands were purified with Geneclean (Bio 101, La Jolla, CA). Single-stranded DNA was prepared with Dynabeads M-280 Streptavidin (Dynal United Kingdom). Chain termination DNA sequencing was done with Sequenase Version 2.0 (U.S. Biochemical). Homology searches were performed with the IFind Sequence Data Bank Searching Program, Version 5.4, Intelligenetics Inc., licensed to ICFR 7145.000392.
19. The nucleotide sequence data can be found in the GenBank/European Molecular Biology Laboratory and DNA Databank of Japan Nucleotide Sequence Databases under the accession number X70980. The exon organization of the mouse *Fcgr1* gene (*17*) is as follows: exon 1, nucleotide (nt) −72 up to and including nt −14; exon 2, from nt −13 to and including nt 7; exon 3, from nt 8 up to and including nt 265; exon 4, from nt 266 up to and including nt 514; exon 5, from nt 515 up to and including nt 799; and exon 6, from nt 800 up to and including nt 1144. Differences between the NOD cDNA sequence and the B10 sequence are at the following nucleotide positions [the equivalent positions in (*17*) are given in parentheses]: at 122 (50) the B10 sequence has T and the NOD sequence has C, resulting in an amino acid

substitution from Val to Ala [nomenclature 122 (50), T → C, Val → Ala]; 207 (135), C → T, 215 (143), C → T, Ala → Val; 224 (152), T → C, Ile → Thr; 231 (159), G → A; 247 (175), C → T, Pro → Ser; 251 (179), A → T, Glu → Val; 261 (189), T → C; 301 (229), A → G, Met → Val; 336 (264), T → G, Asn → Lys; 423 (348), A → G; 448 (373), A → C; 466 (391), C → A, Gln → Lys; 479 (404), A → G, Asp → Gly; 484 (409), G → A, Glu → Lys; 487 (412), G → A, Val → Ile; 542 (467), C → T, Thr → Met; 718 (631), C → T, His → Tyr; 834 (747), G → A; 857 (770), G → A, Arg → His; 864 (777), T → C; 865 (778), G → A, Glu → Lys; 953 (866), C → T, Ser → Leu; and 955 (868), T → G, Leu → Val. In NOD, there is an insertion of 3 nt, AAG, at the 3′-end of exon 3, an insertion of 12 nt, CTTTC-CCTTTAG, at the 3′-end of exon 4, and a deletion of 4 nt, GAGA, after position 996 (910 to 913).
20. M. F. Seldin, T. H. Roderick, B. Paigen, *Mammalian Genome* 1, S1 (1991).
21. J. C. Unkeless, E. Scigliano, V. H. Freedman, *Annu. Rev. Immunol.* **6**, 251 (1988).
22. H. Kikutani and S. Makino, *Adv. Immunol.* **51**, 285 (1992).
23. J. V. Ravetch and J.-P. Kinet, *Annu. Rev. Immunol.* **9**, 457 (1991).
24. K.-P. Lee, K. Amano, J.-W. Yoon, *Diabetes* **37**, 989 (1988); P. Hutchings *et al.*, *Nature* **348**, 639 (1990).
25. L. Shen, P. M. Guyre, C. L. Anderson, M. W. Fanger, *J. Immunol.* **137**, 3378 (1986).
26. H. Nakajima *et al.*, *Immunol. Lett.* **12**, 91 (1986).
27. We designed primers to amplify the transmembrane/cytoplasmic tail (T/C) coding region of *Fcgr1* from genomic DNA of the ICR mouse strain (5′-GTCCCCAGTCATCAGCTCCTG-3′ and 5′-AGAGTTGCATGCCATGGTCCC-3′). PCR reactions (100-μl) were done with biotinylated and nonbiotinylated primers in a Perkin-Elmer Thermocycler for 32 cycles comprising 1.5 min at 94°C, 1 min at 60°C, and 0.5 min at 72°C. Single-stranded DNA was prepared with Dynabeads M-280 Streptavidin. Chain termination DNA sequencing was done with Sequenase Version 2.0.
28. M. Sensi, P. Pozzilli, A. N. Gorsuch, G. F. Bottazzo, A. G. Cudworth, *Diabetologia* **20**, 106 (1981).
29. J. M. H. Debets, J. G. Van de Winkel, J. L. Cueppens, I. E. Dieteren, W. A. Buurman, *J. Immunol.* **144**, 1304 (1990).
30. C. O. Jacob, S. Aiso, S. A. Michie, H. O. McDevitt, H. Acha-Orbea, *Proc. Natl. Acad. Sci. U.S.A.* **87**, 968 (1990).
31. T. Mandrup-Poulsen, K. Bendtzen, C. A. Dinarello, J. Nerup, *J. Immunol.* **139**, 4077 (1987).
32. Y. Ohta, T. P. Stossel, J. H. Hartwig, *Cell* **67**, 275 (1991).
33. D. Baker *et al.*, *J. Neuroimmunol.* **28**, 261 (1990).
34. S. Kataoka *et al.*, *Diabetes* **32**, 247 (1983).
35. The following strains were checked for the presence of the deletion in the cytoplasmic region of *Fcgr1* by PCR (*10*): A/J, AKR/J, B6.PL, BALB/c, high antibody responder Biozzi (AB/H), low antibody responder Biozzi (AB/L), C3H/HeJ, C57BL/6J, C57BL/10SnJ, C57Br/cdJ, C57L/J, Cast/Ei, CBA/J, DBA/2J, ICR, MRL/MpJ-+/+, MRL/MpJ-*lpr/lpr*, NOD, NON, NZB/B1NJ, NZW/lacJ, PL/J, *Mus spretus*/CRC, and SWR/J (*33, 36, 37*). A 184-bp product was obtained from NOD and AB/H, and a 188-bp product was obtained from the other strains.
36. G. Biozzi, D. Mouton, C. Stiffel, Y. Bouthillier, *Adv. Immunol.* **36**, 189 (1984).
37. M. F. Lyon and A. G. Searle, Eds., *Genetic Variants and Strains of the Laboratory Mouse* (Oxford Univ. Press, Oxford, 1989), ed. 2.
38. B10 mice were from the Jackson Laboratory (Bar Harbor, ME), and NOD mice were from Taconic Farm, Germantown, NY. CFA was prepared with heat-killed *Mycobacterium tuberculosis* (strain H37Ra) at a final concentration of 1.0 mg/ml, and an emulsion was made with an equal volume of sterile Dulbecco's phosphate-buffered saline. All mice were injected with 50 μl of CFA in each of the hind feet and boosted with 0.1 ml of CFA in the peritoneal cavity (IP) 14 days later. Flow cytometric analysis was performed 7 to 14 days after the IP injection on either a FACScan or FACStarPLUS (Becton Dickinson). MAb to Mac-1 (Hybritech, San Diego, CA) was used. FITC-conjugated antibody to rat κ (clone MARK-1) and MAb to IgG2a (clone H106.112.52) (AMAC, Westbrook, ME) were used. Phycoerythrin (PE)–conjugated and FITC-conjugated antibody to IgG2a^b (clone 5.7), FITC-IgG2a (clone SF1-1.1), and FITC-IgG3 (IgG3, κ; Pharmingen, San Diego, CA) were used. All antibodies were titrated and used at saturation. All incubations and washes were performed at 4°C. We added propidium iodide to exclude dead cells from the analysis.
39. W. Dietrich *et al.*, *Genetics* **131**, 423 (1992).
40. Linkage was tested in 106 diabetic animals and 89 nondiabetic progeny with insulitis from the (NOD × B10.*H-2^{g7}*)F_1 × NOD backcross and the reciprocal cross, which have been described (*1*). Insulitis was scored as described (*1*). Pair-wise recombination fractions and SEs are given. Genotype frequency differences were evaluated by χ^2 test of independence (1 df).
41. First backcross mice were bred with NOD and B6.PL–*Thy-1^a* and B10.*H-2^{g7}* mice according to the breeding schemes (NOD × B6.PL–*Thy-1^a*)F_1 × B6.PL–*Thy-1^a*, and B10.*H-2^{g7}* × (B10.*H-2^{g7}* × NOD)F_1 and scored for the IgG2a phenotype (*38*). Discordant animals either expressed the phenotype and were B10.*H-2^{g7}* or B6.PL–*Thy-1^a* homozygous or did not express the phenotype and were heterozygous at the marker locus. Marker loci *D3Nds6* (*Il-2*), *D3Nds1*, *D3Nds7* (*Cacy*), *D3Nds8* (*Tshb*), and *D3Nds9* (*Adh-1*) have been described (*1, 9, 15*). Previous marker loci names are given in parentheses. *D3Mit22* has been described (*39*). We ordered marker loci by minimizing double recombinants. Pair-wise recombination fractions and SEs are given. Statistical analysis was by χ^2 test of independence (1 df).
42. NOD.*D3Nds7 D3Nds8* congenic mice were derived from NOD.*D3Nds6 D3Nds8* congenic mice (*11*). The *D3Nds7-D3Nds8* region was made homozygous by selective intercrossing. After six backcross generations, it is expected that 0.8% (~13 cM) of the genome will be of donor origin. The genome of NOD.*D3Nds7 D3Nds8* mice was fingerprinted with microsatellites. With this approach, the number of backcrosses required to produce informative congenic strains is reduced. The following microsatellites were used: *D1Nds1, D1Mit5, D2Mit11, D2Mit14, D2Mit22, D3Nds6, D3Mit6, D3Nds1, D3Mit22, D3Nds7, D3Nds11, D3Nds8, D4Nds3, D4Nds2, Lck, D4Nds13, D5Mit11, D5Nds2, D6Mit14, D7Nds2, D9Mit20, D9Nds3, D10Mit2, D10Nds1, D11Nds14, D11Nds16, D11Nds1, D11Nds17, D11Nds15, D12Mit2, D14Nds4,* and *D19Mit1* (*15, 39*). Only *D3Nds7, Fcgr1,* and *D3Nds8* were of B6.PL–*Thy-1^a* origin.
43. We thank J. Ravetch for discussion, J. Love for assistance, I. Jackson and J. Dorin for preparation of cosmid 6.11, I. Brown and D. Wraith for materials from the high and low antibody responder Biozzi mice, S. Makino and M. Hattori for genomic DNA from ICR mice, and E. Lander and W. Dietrich for primer sequences provided before publication. Supported by the Wellcome Trust, the Medical Research Council as part of the Human Genome Mapping Project, the Juvenile Diabetes Foundation, and the British Diabetic Association.

2 November 1992; accepted 25 January 1993

TECHNICAL COMMENTS

Immuno-PCR with a Commercially Available Avidin System

Antibody-based detection (*1*) and in vitro DNA amplification (*2*) together constitute a system that unifies two revolutionary methods of modern biology. Amplification of an antibody-born DNA label greatly enhances the signal. A method of immuno–polymerase chain reaction (immuno-PCR) was recently described by T. Sano *et al.* (*3*). We have developed an antigen detection system, similar to an enzyme-linked immunosorbent assay (ELISA), that uses a biotinylated antibody and an avidin-biotinylated DNA complex. We use commercially available avidin instead of the streptavidin–protein A–chimera, as proposed by Sano and Cantor (4). Each system has its advantages and drawbacks.

In our system, we prepare tenfold serial dilutions of the antigen to be detected (mouse antibody to apolipoprotein E, Biogenesis, Bournemouth, United Kingdom) in 0.1 M of bicarbonate coating buffer, pH 9.6. Then we immobilize the antigen on microtiter plates (Maxisorp, Nunc, Roskilde, Denmark) in a volume of 50 μl at concentrations of 1 μg/ml to as little as 10 femtograms per milliliter (fg/ml) by incubation overnight at 4°C. Wells are then washed three times with 200 μl of phosphate-buffered saline (PBS), pH 7.4, and blocked with bovine serum albumin (BSA) (10 g/liter in PBS) for 2 hours. After three additional washings with PBS, biotinylated goat antibody to mouse immunoglobulin G (IgG) is added at 250 pg/ml in PBS that contains 0.01% (v/v) Tween 20 (PBS-Tween) and 1 g/liter BSA for 1 hour.

Avidin-biotinylated DNA complex is prepared by adding 30 μl of avidin preparation (component B of the ABC system from Vector Laboratories, Burlingame, California) and 5 μl of a biotinylated 479-bp PCR product, which encompasses apolipoprotein B complementary DNA (cDNA) nucleotides 10354 to 10832 (5), to 10 ml of PBS and then incubating the mixture for 30 min.

Unbound biotinylated goat antibody to mouse IgG is removed from the microtiter wells by five washings with PBS-Tween. Then 100 μl of avidin-biotinylated DNA complex is loaded and incubated for 30 min. Finally, wells are washed five times with 200 μl of PBS-Tween and three times with distilled water. A 50-μl PCR mixture